

RESEARCH PAPER

 OPEN ACCESS

Position-dependent activity of CELF2 in the regulation of splicing and implications for signal-responsive regulation in T cells

Sandya Ajith^{***}, Matthew R. Gazzara^{*}, Brian S. Cole[#], Ganesh Shankarling[§], Nicole M. Martinez[¶], Michael J. Mallory, and Kristen W. Lynch

Department of Biochemistry and Biophysics, University of Pennsylvania Perelman School of Medicine, Philadelphia, PA, USA

ABSTRACT

CELF2 is an RNA binding protein that has been implicated in developmental and signal-dependent splicing in the heart, brain and T cells. In the heart, CELF2 expression decreases during development, while in T cells CELF2 expression increases both during development and in response to antigen-induced signaling events. Although hundreds of CELF2-responsive splicing events have been identified in both heart and T cells, the way in which CELF2 functions has not been broadly investigated. Here we use CLIP-Seq to identify physical targets of CELF2 in a cultured human T cell line. By comparing the results with known functional targets of CELF2 splicing regulation from the same cell line we demonstrate a generalizable position-dependence of CELF2 activity that is consistent with previous mechanistic studies of individual CELF2 target genes in heart and brain. Strikingly, this general position-dependence is sufficient to explain the bi-directional activity of CELF2 on 2 T cell targets recently reported. Therefore, we propose that the location of CELF2 binding around an exon is a primary predictor of CELF2 function in a broad range of cellular contexts.

ARTICLE HISTORY

Received 5 February 2016
Revised 31 March 2016
Accepted 4 April 2016

KEYWORDS

Alternative splicing; CELF2;
CLIP-Seq; LEF1; MKK7; RNA
map

Introduction

Alternative splicing of pre-mRNAs is typically controlled by binding of proteins along a nascent transcript that in turn direct the splicing machinery to include or skip specific exons in the splicing process.¹ Such regulated inclusion of exons, or portions thereof, generates protein diversity, controls protein expression and plays a crucial role in processes like the epithelial-to-mesenchymal transition, regulation of action potentials, heart development and regulation of T cell development and function in the immune system.^{2–5} One RNA binding protein (RBP) that has been particularly linked to alternative splicing in many of these developmental and differentiation processes is CELF2.^{6–10}

CELF2 is part of the CUGBP, ELAV-Like Family (CELF) of proteins of which there are 6 members.^{9,11} All members of this family are characterized by 3 RNA Recognition Motifs (RRMs). RRM1 and 2 lie at the N terminus of the protein, followed by a linker domain and a C-terminal RRM3. The six CELF proteins exhibit high sequence similarity in their RRM domains, but diverge in the linker domain.^{9,11} The CELF proteins also differ

in their expression patterns. CELF3–6 are largely restricted to neurons and a few other tissues, while CELF1 and CELF2 are present in most tissues but vary in expression during development and differentiation.¹¹ CELF1 and CELF2 are both highly expressed in the fetal heart but show a marked reduction in expression during post-natal development.^{10,12} By contrast, CELF2 expression increases during thymic development and upon activation of mature T cells, while CELF1 expression remains constant.⁷ Consistent with the high degree of sequence conservation within the CELF family, several studies have shown that the RRM3s of all CELF proteins bind UG-rich sequences; however, the 6 CELF proteins exhibit different activities as a result of differential expression and/or differences in their linker domain.^{11,13–15} For example, CELF1 and CELF2 share similar activities in heart development, but are expressed in mutually exclusive territories in the eye and CELF1 does not substitute for the splicing regulatory activities of CELF2 in T cells.^{7,10,16}

As is typical for RBPs, CELF2 has been implicated in the regulation of several steps in RNA biogenesis, including

CONTACT Kristen W. Lynch  klync@mail.med.upenn.edu


*These authors equally contributed to this work.

**Current addresses: Arcus Medica, Philadelphia, PA, USA

†Current addresses: Institute for Biomedical Informatics, University of Pennsylvania Perelman School of Medicine, Philadelphia, PA, USA

‡Current addresses: Bristol-Myers Squibb, Pennington, NJ, USA

§Current addresses: Department of Biology, MIT, Cambridge, MA, USA

 Supplemental data for this article can be accessed on the publisher's website.

Published with license by Taylor & Francis Group, LLC © Sandya Ajith, Matthew R. Gazzara, Brian S. Cole, Ganesh Shankarling, Nicole M. Martinez, Michael J. Mallory, and Kristen W. Lynch

This is an Open Access article distributed under the terms of the Creative Commons Attribution-Non-Commercial License (<http://creativecommons.org/licenses/by-nc/3.0/>), which permits unrestricted non-commercial use, distribution, and reproduction in any medium, provided the original work is properly cited. The moral rights of the named author(s) have been asserted.

alternative splicing, translation control and mRNA stability.¹¹ In the case of alternative splicing, CELF2 has been shown to act as both an activator and repressor of exon inclusion. An example of CELF2 activating exon inclusion is the regulation of Cardiac Troponin T (cTNT)'s exon 5, which is preferentially included in embryonic striated muscle but excluded in adult tissue.⁹ The isoforms created from the alternative splicing of exon 5 confer different contractile properties to the muscle tissue.¹⁷ Similarly, in activated T cells CELF2 promotes inclusion of exon 6 of the LEF1 transcription factor, resulting in an isoform that is optimized to induce TCR- α expression.⁷ On the other hand, we recently demonstrated that CELF2 represses inclusion of exon 2 of the MAP Kinase MKK7, thereby promoting the ability of MKK7 to associate with its substrate JNK.¹⁸ Thus CELF2-dependent alternative splicing of MKK7 amplifies JNK signaling in activated T cells.

Interestingly, previous studies of known muscle and cardiac-relevant CELF2 target genes have suggested that CELF2 exerts distinct effects on exon inclusion depending on the location of its binding. For example, CELF2 binds upstream of several exons it is known to repress, including exon 9 of CFTR, NMDAR1 exon 5 (N1), α actinin exon NM and CELF2s own exon 6.¹¹ In the case of CFTR exon 9, it has been shown that binding of CELF2 to a UG-rich sequence within the polypyrimidine tract (PPT) upstream of exon 9 represses exon inclusion by displacing binding of constitutive splicing factor U2AF65 from the PPT.¹⁵ By contrast, CELF2 enhances inclusion of cTNT exon 5 by binding downstream of the exon and stabilizing U2 snRNP binding at the upstream 3' splice site.¹⁹ However, it has not been established whether these individual examples of position-dependent activity represent a general predictive feature of CELF2 activity in alternative splicing.

Global sequencing studies and MS2 tethering assays have revealed that a significant number of splicing factors do show pervasive position-dependent activity, including Nova, RbFox2, TIA-1, MBNL1/2, ESRP1/2.¹ However, other RNA binding proteins, such as hnRNP L, lack any generalizable correlation between binding position and differential activity.²⁰ In addition, despite the evidence for position-dependent activity of CELF2 in cardiac and muscle tissue, the best characterized targets of CELF2-dependent regulation in T cells, LEF1 exon 6 (LEF1-E6) and MKK7 exon 2 (MKK7-E2), do not appear to fit a simple position-determined pattern. The CELF2-dependent regulation of LEF1-E6, as well as MKK7-E2, requires intronic sequences on both sides of these exons; however CELF2 enhances LEF1-E6 while repressing MKK7-E2.^{7,18}

Here we investigate the correlation between CELF2 binding and function in alternative splicing by using CLIP-Seq to identify transcriptome-wide binding of CELF2 in a T cell line in which we have previously identified a large-scale set of functional targets of CELF2-dependent splicing.⁶ This analysis reveals a consistent and generalizable relationship between the position of CELF2 binding relative to a variable exon and the effect of CELF2 on splicing outcome. This relationship between binding and function is consistent with previous studies; namely CELF2 represses inclusion of downstream exons and enhances inclusion of upstream exons. Based on this general trend, we then further investigated the apparent discrepancy in

CELF2 binding and function observed for LEF1-E6 versus MKK7-E2. Strikingly, we find that while intron elements on either side of both LEF1-E6 and MKK7-E2 are required for CELF2 regulation, CELF2 binds preferentially to one side or the other to regulate exon inclusion in a manner that is entirely consistent with the position-dependent activity observed for other genes. Therefore, we conclude that position-dependent splicing regulation is a general feature of CELF2 splicing activity across many cell types and can be used to predict CELF2 function.

Results

We have previously identified approximately 300 CELF2-regulated splicing events in unstimulated and PMA-stimulated Jurkat T cells.⁶ To gain a comprehensive comparison between the binding and function of CELF2 we therefore used this same Jurkat system to interrogate the transcriptome-wide binding of CELF2 by CLIP-Seq. Briefly, we isolated biologic triplicate samples of Jurkat cells that had either been maintained in media alone or stimulated in culture with the phorbol-ester PMA, which mimics the diacylglyceride-dependent arm of T cell signaling.²¹ Direct protein-RNA interactions were fixed in living cells by treatment with UV light, which induces covalent cross-links between proteins and the RNAs to which they are directly bound.²² Cells were then lysed, RNA was fragmented to a size range of 30–110 nts, and CELF2-RNA complexes were stringently purified using a well-described antibody specific for endogenous human CELF2.⁷ This antibody efficiently precipitated all detectable CELF2 (Fig S1A), without any appreciable cross-contamination from CELF1 or other RBPs known to bind to similar sequence motifs (PTB, TIA1, HuR, Fig S1A). Following isolation of the CELF2-RNA complexes from cells, RNAs were released from the protein, tagged with RNA linkers and subjected to high throughput sequencing (see Methods).

CELF2-RNA interaction profiles in T cells

From the 3 biologic replicates of CLIP from unstimulated and stimulated Jurkat cells we obtained a total of ~120 million reads mapping unambiguously to the human genome, distributed equally between the 2 conditions (Fig. 1A). Removal of PCR duplicates from these reads resulted in 7.8 million unique alignments or “tags” (Fig. 1A). Notably, over 80% of the unique alignments fall within RefSeq annotated sequence (Fig. 1A), suggesting that the primary role of CELF2 in these T cells relates to the processing of transcribed RNAs. Using a peak calling method we have previously described^{23,24}, we identified ~50,000 significant peaks of CELF2 binding in each cell growth condition from these RefSeq-mapped reads (Fig. 1A). Importantly, we note that there is >60% overlap between CELF2 peaks identified in unstimulated and stimulated cells (Fig S1B), with over 90% of peaks overlapping with a region containing at least 2 tags in the other condition and greater than 80% correlation between the number of tags in each peak between the 2 condition (Fig. S1C). Thus the majority of binding sites for CELF2 remain unchanged despite the 2-3-fold increase in CELF2 protein expression that occurs upon stimulation of Jurkat cells.

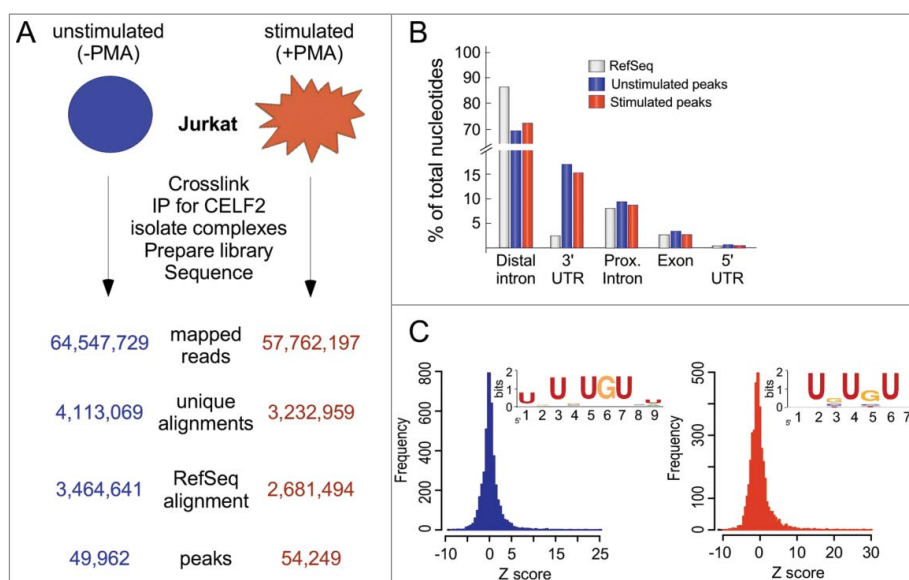


Figure 1. CELF2 binds similarly in unstimulated and stimulated Jurkat T cells to UGU-rich regulatory regions. (A) Basic workflow and read count of CLIP-Seq analysis of CELF2 in unstimulated (blue) or stimulated (red) JSL1 Jurkat cells. Mapped reads (reads that aligned to one and only one position in the hg19 build of the human genome), unique alignments (reads after PCR duplicates removed), RefSeq alignments (reads falling within RefSeq transcriptome annotation), and final CLIP-Seq peaks are displayed. (B) Barplot of the fraction of nucleotides covered by CELF2 CLIP-seq peaks in unstimulated and stimulated Jurkat cells occupying each of 5 categories of annotation, compared to percentage of RefSeq sequence space covered by each annotation. (C) Unstimulated (left, blue) and stimulated (right, red) CELF2 CLIP-seq peaks were permuted 100 times within the RefSeq transcripts to which they align and hexamer frequencies within the actual CLIP-seq peaks were compared to the mean and standard deviation for that hexamer across the 100 iterations of independent permutations. The Z-score is reported as the number of standard deviations away from the mean permuted frequency, with positive values denoting enrichment and negative values depletion. Inset: a composite motif logo generated from multiple sequence alignment of the top 20 hexamers by Z score.

As expected from the general tendency of RBPs to function in pre-mRNA splicing by localizing near splice sites, CELF2 binding sites (i.e. CLIP peaks) are more biased to proximal introns (within 300nt of an exon) and exonic sequence vs. distal introns when compared to the total sequence space (Fig. 1B and see below). Interestingly, CELF2 binding sites are also enriched in 3' UTR exons (Fig. 1B). Although we have not pursued investigation here of the functional implication of 3' UTR binding of CELF2, CELF2 has been shown previously to bind the 3' UTRs of the *Cox-2* and *MCL1* genes and regulate their expression.¹¹ Finally, consistent with previous reports of the binding preference for CELF proteins, we observe a marked bias toward UGU trinucleotides in both unstimulated and stimulated CELF2 peaks (Fig. 1C). The similarity in the logo derived from the top 20 most enriched hexamers from unstimulated and stimulated cells (Fig. 1C, insert), is consistent with the overlap in binding sites between these 2 conditions.

Given our recent identification of CELF2-regulated exons in Jurkat cells, we sought to further investigate the correlation between the location of CELF2 binding and its impact on splicing of variable exons. Given the high degree of overlap of binding sites in unstimulated and stimulated cells we combined these datasets to increase the number of events surveyed. We first reanalyzed the location of CELF2 peaks as in Fig. 1B with focus on the sequence space surrounding CELF2-regulated alternative (A) exons. Strikingly we find significant enrichment of CELF2 binding in the 300 nucleotides upstream of exons that it represses and downstream of exons that are CELF2-enhanced, with little enrichment of binding of CELF2 at more distal locations (Fig. 2A). The significant correlation between proximal CELF2 binding location and function is further observed upon mapping the CLIP peaks across the

sequences surrounding CELF2-regulated exons (Fig. 2B) and comparing the distribution of splicing changes relative to binding location (Fig. S2A). The biologic importance of CELF2-binding is underscored by the strong phylogenetic conservation of sequences in the CELF2-bound regions around the exons it regulates (Fig. 2C), as well as CELF2-binding sites in general (Fig. S2B). In addition, gene ontology analysis reveals enrichment of distinct protein functions among the genes with CELF2 bound in proximal intronic regions (I1A, A12) versus those with binding in locations that do not correlate with splicing function (other) (Fig. 2D, Table S1). Together, these data suggest that CELF2-dependent regulation of exon inclusion is biologically relevant and strongly driven through direct binding of CELF2 to pre-mRNA substrates. Moreover, our data demonstrate that the functional consequence of CELF2 in regulating splicing globally correlates with the location of its binding relative to the exon it controls, suggesting a generalized position-dependent activity of CELF2 in splicing regulation.

Position-dependent binding and function of CELF2 to LEF1

Curiously, the 2 best characterized targets of CELF2-dependent splicing in T cells have features that appear to contradict the position-dependence we observe for other genes. Specifically, both LEF1-E6 and MKK7-E2 are regulated by CELF2 and intronic sequences located on both sides of the alternative exon^{7,18}; yet when CELF2 expression is increased upon T cell activation LEF1-E6 is enhanced (Fig. 3A, B) while MKK7-E2 is skipped (Fig. 3C).^{7,18} To determine if CELF2 regulation of these exons does indeed conform to the position-dependent activity we observe for other exons, or how this regulation may differ,

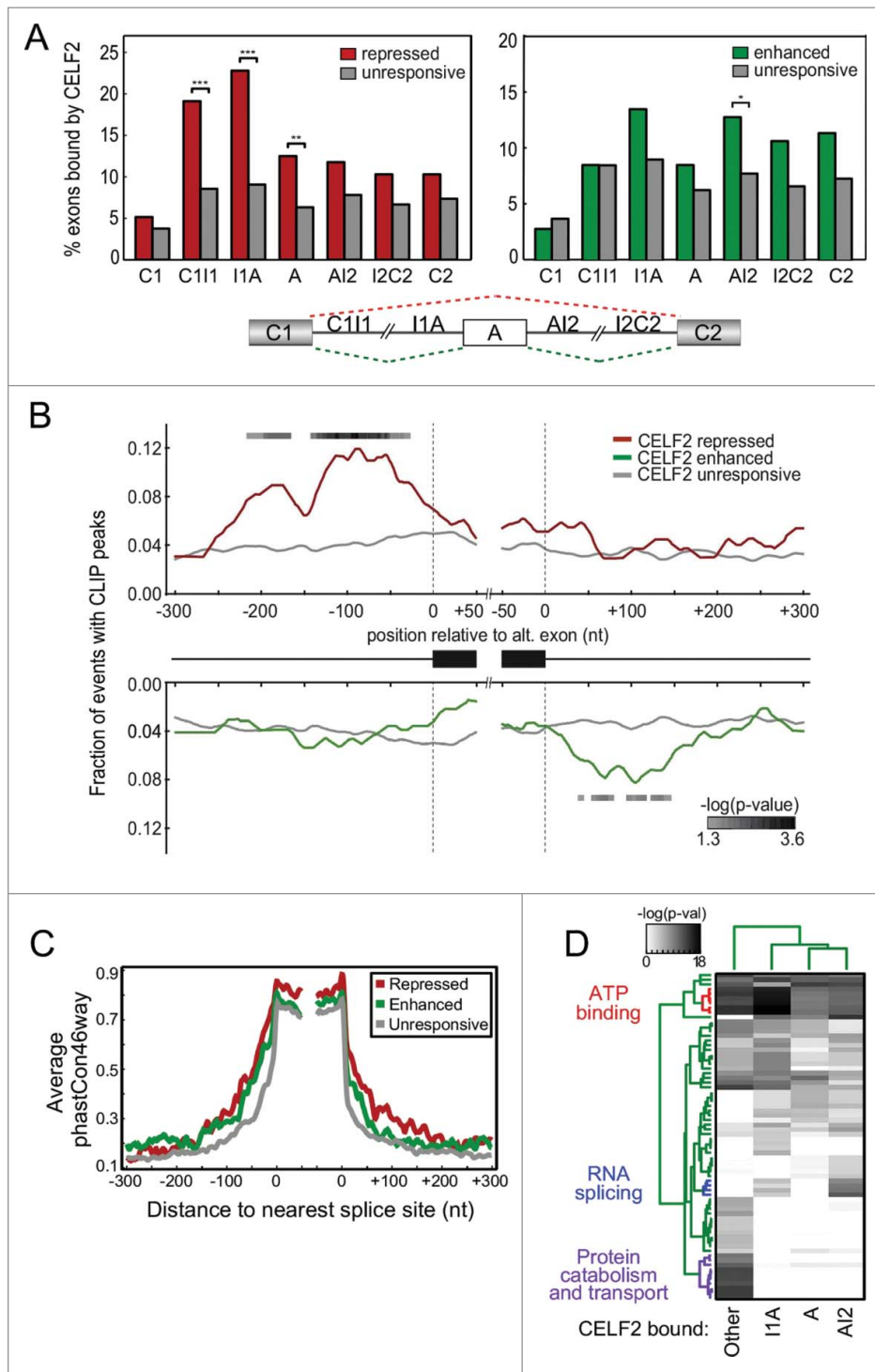


Figure 2. Binding position of CELF2 correlates with functional outcome on splicing. (A) Barplots displaying the fraction of CELF2 repressed exons (left, red, $n = 135$) or CELF2 enhanced exons (right, green, $n = 140$) with a CLIP peak in each given splicing-relevant region represented in the inset, compared to the set of exons that are unresponsive to CELF2 depletion (gray, $n = 903$) (Binomial test 2-tailed p -value < 0.05 *; < 0.01 **; < 0.001 ***). (B) RNA map shows the per nucleotide fraction of CELF2 repressed exons (top, red) or CELF2 enhanced exons (bottom, green) with a CLIP-seq peak proximal to regulated exons' splice sites, compared to the set of unresponsive exons (gray). Positions of significant difference are indicated by gray scale squares with intensities corresponding to p -values ($-\log_{10}$ scale) indicated in inset (Fisher's exact 2-tailed p -value < 0.05 or $-\log(p)$ > 1.3). Fractions were smoothed using a 11-nt running average centered on each position. (C) Per nucleotide mean conservation (phastCons46way, placental mammals) in regions proximal to splice sites for sets indicated in legends compared to a set of expressed alternative exons queried by RASL-seq. (D) Clustering of significantly enriched GO terms (Bonferroni corrected p -value < 0.05) in genes containing CELF2 peaks proximal to exons (300 nt upstream (I1A), 300 nt downstream (AI2), or within exons (A)) or bound elsewhere on transcripts ("other," e.g. distal intronic or UTR regions).

we carried out a detailed analysis of the binding and activity of CELF2 in these genes.

We first focused on LEF1 exon 6 (LEF1-E6). In previous studies we have identified 2 elements that control the inclusion

of LEF1-E6. These two elements include the USE, a 60 nt sequence coincident with the polypyrimidine tract upstream of LEF1-E6, and the DSE, a 120 nt sequence located about 40 nt downstream of the 5ss of LEF1-E6⁷ (Fig. 4). Both of these

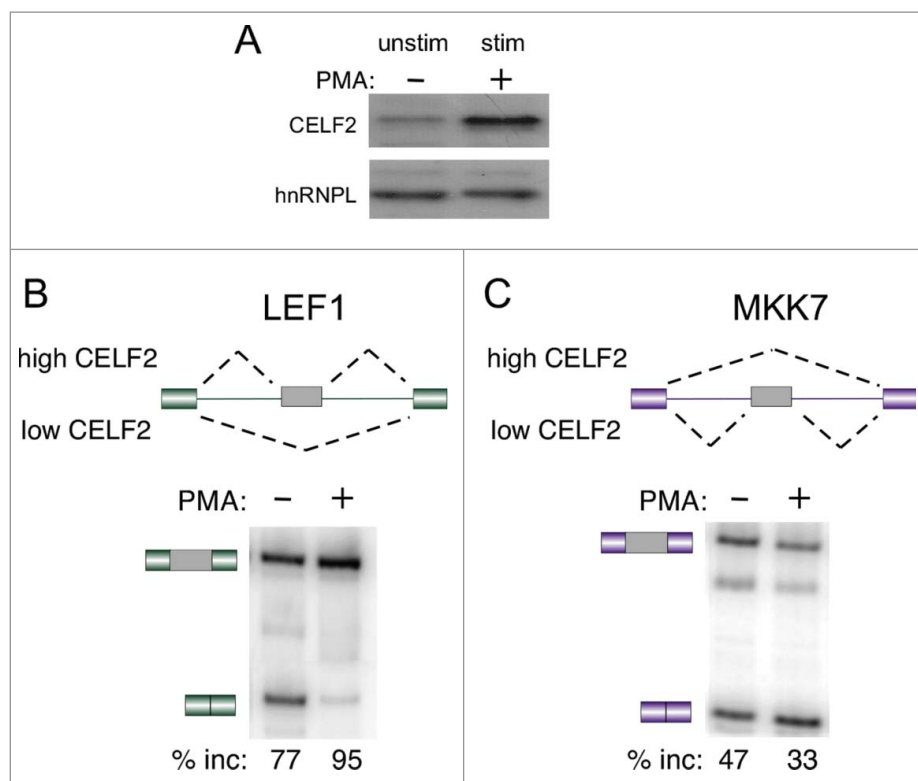


Figure 3. Differential response of LEF1-E6 and MKK7-E2 to increasing expression of CELF2 upon T cell stimulation (A) Western blot of CELF2 in unstimulated (-PMA) or stimulated (+PMA) Jurkat cells. HnRNP L is used as a loading control. (B) Schematic of LEF1 exons 5–7 (top) and representative RT-PCR (bottom) of showing splicing of E6 in the endogenous LEF1 transcript in Jurkat cells $-/+$ PMA. % inclusion (% inc) of the variable exon is the average from $n \geq 4$ independent experiments. (C) Same as panel B but for MKK7 exons 1–3.

sequences in isolation bind to CELF2 and function together to confer CELF2 dependent regulation of LEF1-E6.⁷ Moreover, we detect peaks of CELF2 binding to both of these sequences in the CLIP data. However, we have not previously tested the splicing regulatory activities of these sequence elements in isolation. We therefore constructed minigenes that individually interrogate the regulatory activity of the USE and DSE by substituting heterologous intron sequences for the USE and DSE, keeping intact any sequences required for the basic splicing machinery such as the polypyrimidine tract. Interestingly, we find that removal of the DSE reduced splicing to LEF1-E6 *in vitro* (Fig. 4A), which corresponds to decreased inclusion of LEF1-E6 in a 3-exon minigene assay in Jurkat cells (Fig. 4B). Furthermore, this splicing-enhancing effect of the DSE was independent of the presence or absence of the USE, as we observe a similar reduction of splicing upon substitution of the DSE in constructs that contain the USE (USE/DSE vs USE/alt120, Fig. 4A, 4B), lack the USE (Δ /DSE vs Δ /alt120, Fig. 4A) or have a heterologous polypyrimidine tract in place of the USE (alt60/DSE vs alt-both, Fig. 4B). Conversely, removal (Δ) or substitution (alt60) of the USE resulted in an increase in splicing and inclusion of LEF1-E6, again regardless of the presence or absence of the DSE (Fig. 4A, B). Therefore, consistent with the position-dependent activity of CELF2 inferred from the CLIP-Seq studies, the presence of the CELF2-binding upstream of LEF1-E6 (USE) represses exon usage, while the CELF2-binding element downstream of LEF1-E6 (DSE) activates splicing to this exon.

In order to further substantiate that position relative to the exon is the primary determinant of the differential activity of the DSE and USE we moved the DSE upstream. First we shortened the downstream intron to enable some detection of inclusion in the absence of the downstream DSE. In this background, addition of the DSE upstream of the USE further repressed exon inclusion (Fig. S3A), again consistent with the location of the DSE being the primary determinant of its function and with a model in which increased binding of CELF2 upstream of an exon results in increased repression. We cannot do the converse experiment of moving the complete USE downstream, as this sequence not only binds CELF2 but also contains an active 3' splice site. Therefore, to specifically test the functionality of CELF2 binding downstream of LEF1-E6, we substituted the DSE with a 21 nucleotide sequence that has previously been shown to bind CELF2 with high affinity²⁵ (UGUU). CELF2 binds to the UGUU element in a copy number-dependent manner, such that 4 copies of UGUU approach a similar affinity for CELF2 as does the wildtype DSE or USE (Fig. S3B). Strikingly, we observe a copy number-dependent enhancing activity of the UGUU element on splicing, in which inclusion of LEF1-E6 is proportional to the number of UGUU elements (and thus affinity of CELF2) (Fig. 4C).

From the above data we conclude that CELF2 regulates inclusion of LEF1-E6 through the USE and DSE in a position-dependent manner that is consistent with behavior we observe for CELF2 on a transcriptome-wide level (Fig. 2). However, we note that the position-dependent activity of CELF2 does not immediately explain the increase in LEF1-E6 inclusion that is observed upon the increasing CELF2 expression in activated or maturing T cells, as

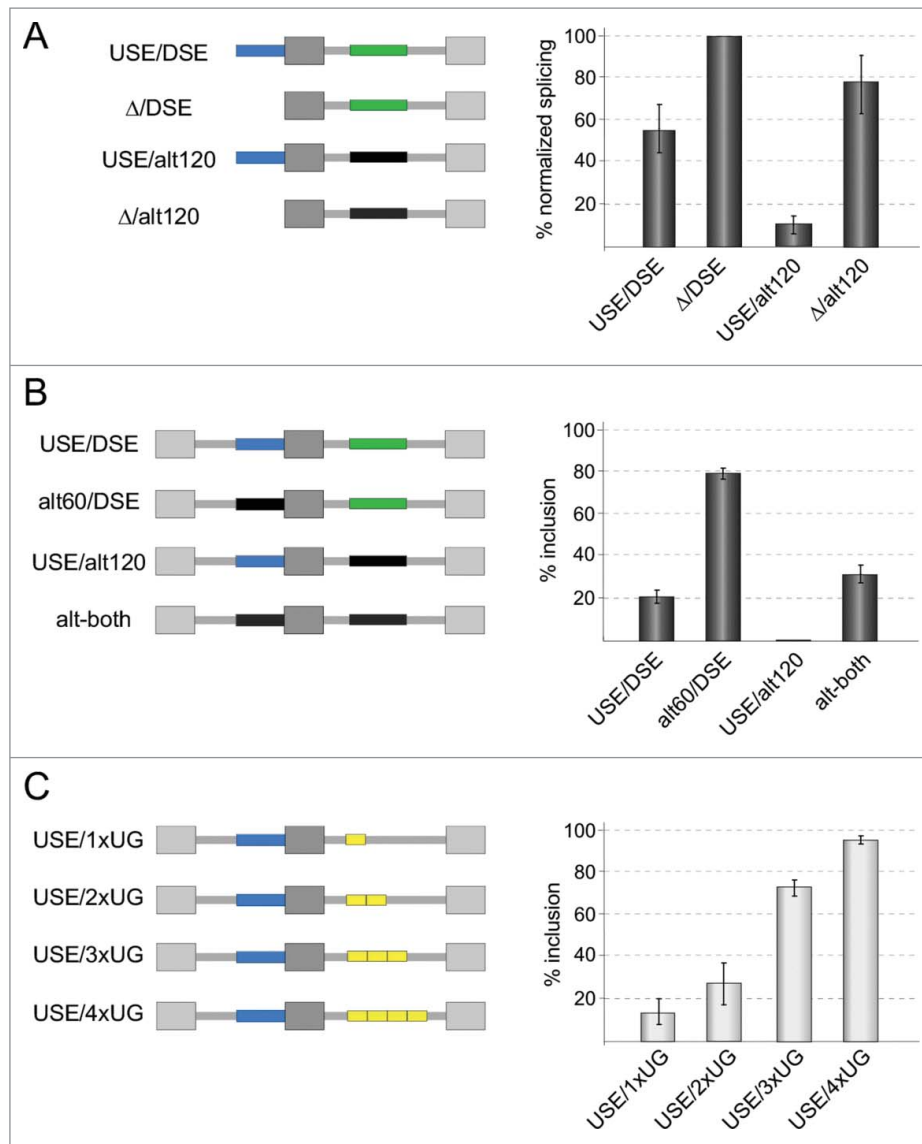


Figure 4. Position dependent activity of CELF2-binding sites in regulation of LEF1-E6. (A) Percentage of total in vitro splicing activity observed for single-intron variants of LEF1 indicated on left. Blue, USE; Green, DSE; Black, heterologous sequence from human- β globin to substitute for USE or DSE; Gray, standard human- β globin splicing backbone. (B) Percent inclusion of LEF1-E6 in 3-exon minigenes stably expressed in Jurkat cells. Splicing analyzed by RT-PCR as described in Methods. Colors for minigene schematics are the same as in panel A. (C) Percent inclusion of LEF1-E6 in 3-exon minigenes stably expressed in Jurkat cells, as in panel B except that DSE was substituted by 1-4 copies (1xUG-4xUG) of the “UGUU” sequence GUGCUUUUCUGUUGUUGUUGU. All data is the average of at least 3 independent experiments. Representative RT-PCR gels for panels A-C are shown in Fig. S3C

both the USE and DSE in isolation bind to CELF2 with equal affinity (Fig. S3B). We considered the possibility, therefore, that the USE and DSE have differing abilities to recruit CELF2 within the context of the more complete LEF1 sequence. To test this possibility, we carried out UV crosslinking of proteins extracted from unstimulated or stimulated Jurkat cells with RNAs derived from the minigenes that individually lack the USE and/or DSE. Strikingly, we find that a protein species of the size of CELF2 binds considerably more strongly to the wildtype or alt60/DSE in extracts from stimulated cells than it does in extracts from unstimulated cells (Fig. 5A). By contrast, only minimal binding to this species is observed in either extract using the USE/alt120 or alt-both RNAs (Fig. 5A). We confirmed the identity of this protein as CELF2 using immunoprecipitation with specific antibodies (Fig. 5B). In the immunoprecipitation experiment it is again apparent that CELF2 binding to RNAs containing the DSE is enhanced upon

stimulation. By contrast, the RNA containing only the USE exhibits a similar residual association with CELF2 in both unstimulated and stimulated extracts, while there is no apparent association of CELF2 with the alt-both construct. These results suggest that while CELF2 can bind to both the USE and DSE, in the broader context of the LEF1-E6 splicing substrate either the sequence or protein landscape is such that CELF2 preferentially binds to the DSE upon increased protein expression in stimulated cells. Importantly, increased binding of CELF2 to the DSE upon stimulation is coincident with increased enhancement of LEF1-E6 inclusion, and thus is consistent with the position-dependent activity of CELF2.

To further confirm that CELF2 is indeed driving the increase in LEF1-E6 inclusion in a stimulation-specific manner we used shRNAs to deplete CELF2 in unstimulated and stimulated cells (Fig. 5C). We have previously shown that knockdown of CELF2 reduces the inclusion of LEF1-E6 in

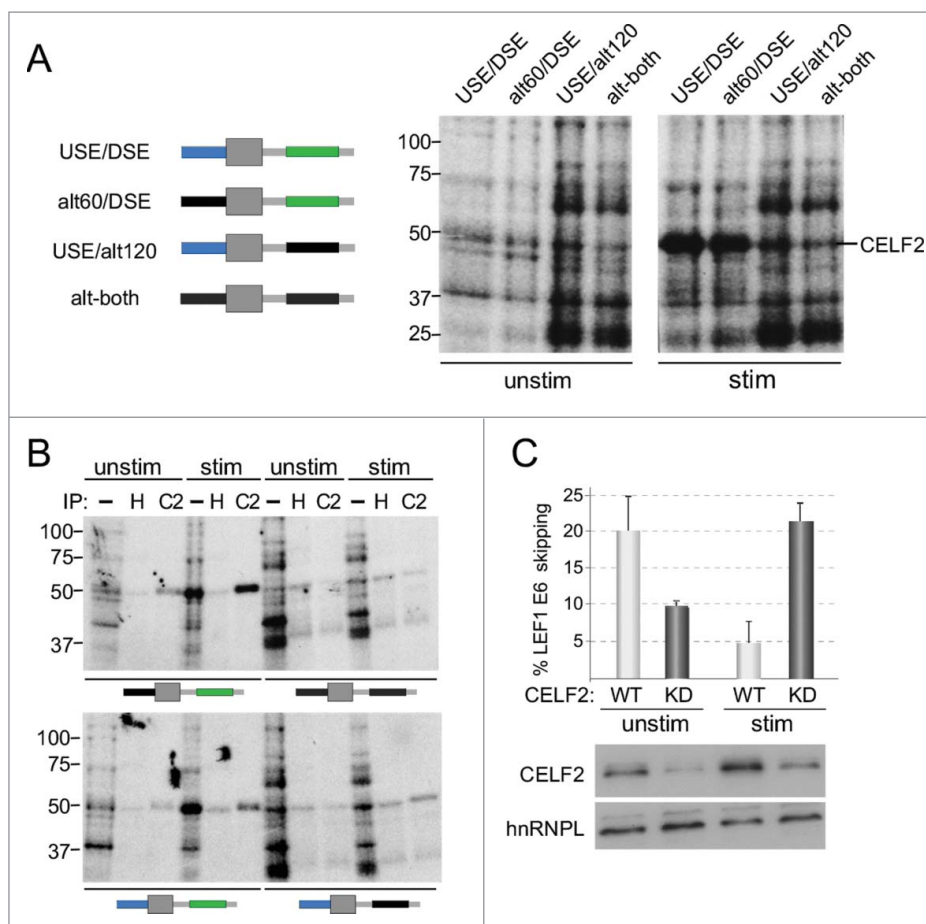


Figure 5. Differential inclusion of LEF1-E6 in unstimulated and stimulated cells is consistent with differential binding preference of CELF2. (A) UV crosslinking (right) of RNAs shown on left with nuclear extract from unstimulated or stimulated Jurkat cells. Blue, USE; Green, DSE; Black, heterologous sequence from human- β globin to substitute for USE or DSE; Gray, standard human- β globin splicing backbone. Position of CELF2 species and molecular weight standards are indicated. (B) UV crosslinking of RNAs indicated as in panel A. -IP is total reaction, IP: H and C2 indicate species isolated by immune-precipitation with antibodies specific for hnRNP H (H) or CELF2 (C2). Note that hnRNP H and CELF2 both migrate at approximately 50 KDa. (C) Quantification (as in Fig 3, $n \geq 3$) of inclusion of exon 6 in the endogenous LEF1 gene in wildtype (WT) cells or those depleted for CELF2 by shRNA (KD, see Methods) cultured under unstimulated or stimulated conditions. Below graph is a western blot showing depletion of CELF2 relative to hnRNPL as loading control.

stimulated cells,⁷ but we had not specifically investigated differential effects of CELF2 expression in unstimulated cells. Remarkably, we find that while knockdown of CELF2 in stimulated cells increases skipping of LEF1-E6 as expected, in unstimulated cells knockdown of CELF2 has the opposite effect, namely decreasing exon skipping. These results demonstrate that in unstimulated cells, in which CELF2 binds to the USE at least as well as it does to the DSE, CELF2 represses LEF1-E6. However, upon stimulation CELF2 preferentially binds to the DSE and its activity is flipped to being an enhancer of LEF1-E6 inclusion. Therefore, a change in CELF2 binding position, together with position-dependent activity, can account for the observed differential regulation of LEF1-E6 by CELF2 under changing protein concentrations.

CELF2 binds upstream of MKK7-E2 to repress exon usage

A second exon that we have shown to be under control of CELF2 upon T cell stimulation is MKK7-E2. Similar to LEF1-E6, MKK7-E2 is flanked by intronic regulatory elements that together bind CELF2. However, unlike LEF1-E6, inclusion of MKK7-E2 is repressed upon stimulation (Fig. 3C), and

knockdown of CELF2 increases MKK7-E2 inclusion in both unstimulated and stimulated cells (Fig. 6A).¹⁸ Notably, in our previous studies we had only investigated the binding of proteins to an RNA that contained both the upstream and downstream regulatory elements of MKK7-E2. Both the upstream and downstream intronic elements have UG-dinucleotides that represent putative CELF2 binding sites (Fig. 6B); however, we detect no CELF2 CLIP peaks in the vicinity of MKK7-E2, perhaps due to low expression of the mRNA. Therefore, to determine if CELF2 binds preferentially to one or the other intron we carried out UV crosslinking on RNAs corresponding to just the upstream or downstream introns separately. Surprisingly, we find that the upstream intronic sequence on its own binds to CELF2, while the downstream sequence does not (Fig. 6C, D). The preferential binding of CELF2 to the upstream intron is further revealed by the ability of the upstream, but not downstream, sequence to competitively titrate binding of CELF2 away from the complete MKK7-E2 substrate, which contains both introns (Fig. S4). We note, however, that the downstream intronic element appears to control the extent of the signal-responsive change in CELF2 binding, in that CELF2 binding is greater in stimulated than unstimulated extracts only in the presence of both intronic elements (Fig. 6C-E). While

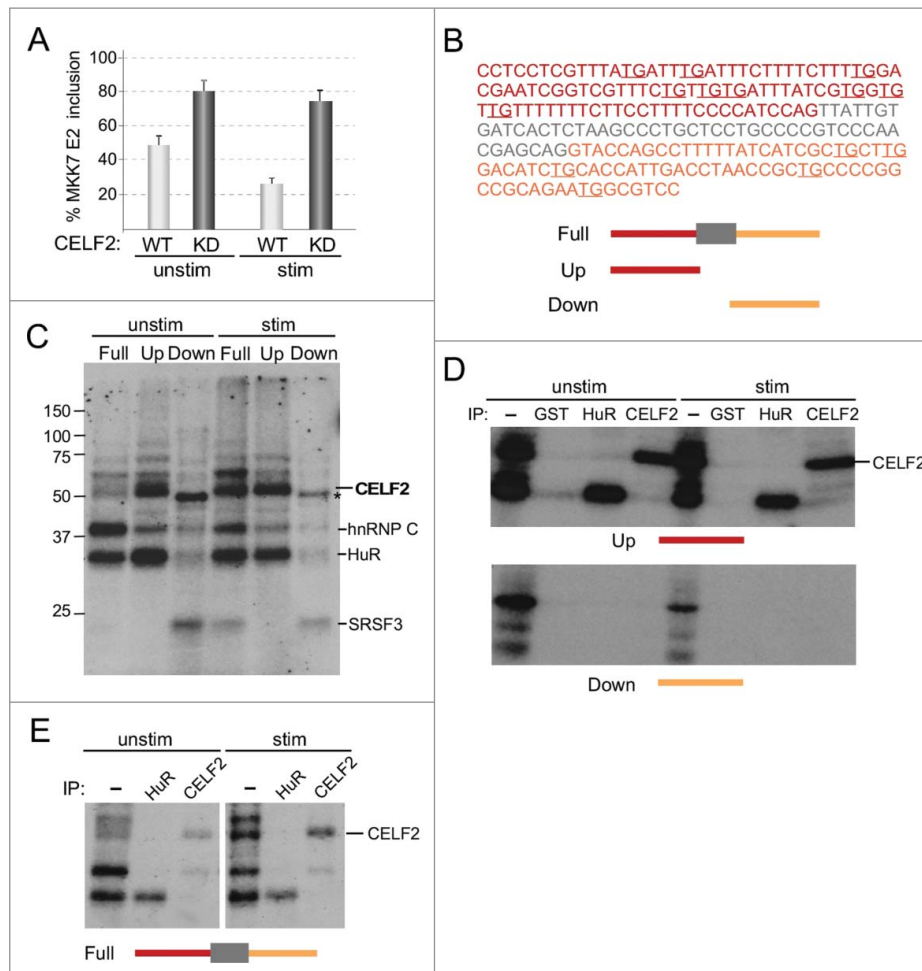


Figure 6. Stimulation-induced repression of MKK7-E2 is consistent with position-dependent activity of CELF2. (A) Quantification (as in Fig. 3, $n \geq 3$) of inclusion of exon 2 in the endogenous MKK7 gene in wildtype (WT) cells or those depleted for CELF2 by shRNA (KD, see Methods) cultured under unstimulated or stimulated conditions as in Fig. 5C. (B) Sequence of MKK7-E2 (gray) and immediate upstream (red) and downstream (orange) intronic sequence shown to be necessary and sufficient for stimulation-induced repression of MKK7-E2.¹⁸ Simplified schematics used in other panels shown at bottom. (C) UV crosslinking of RNAs from panel B with nuclear extract from unstimulated or stimulated Jurkat cells. Position of molecular weight standards are indicated, as well as CELF2, hnRNP C, HuR and SRSF3 as determined previously¹⁸ and in panels D-E. (D) UV Crosslinking of RNAs indicated as in panel B with the Up and Down RNAs (panel B). -IP is total reaction, IP: GST, HuR and CELF2 are following immunoprecipitation with antibodies specific for the indicated proteins. GST is used as a negative control for non-specific interaction, while HuR serves as a positive control for equal binding/IP. Position of CELF2 is indicated. (E) UV Crosslinking of RNAs indicated as in panel B with the Full RNA (panel B). -IP is total reaction, IP: HuR, CELF2, hnRNP C and U2AF65 are following immunoprecipitation with antibodies specific for the indicated proteins. Position of CELF2 is indicated.

additional proteins also bind to the MKK7 introns, including hnRNP C, HuR and SRSF3, we have previously shown these proteins to have little or no impact on the splicing of MKK7-E2.¹⁸ By contrast, the dependence on the downstream element to control binding of CELF2 to the upstream element provides a mechanistic explanation for why both sequences are required for the functional change in splicing upon stimulation. Thus, the pattern and functional outcome of CELF2 binding to MKK7 is again entirely consistent with the general position-dependent activity of CELF2, with binding of CELF2 upstream of MKK7-E2 repressing inclusion of this exon.

Discussion

Comparison of the binding and function of splicing regulatory factors around the exons which they control has greatly informed our understanding of the differential activities of these RNA binding proteins. In some instances, the functional consequence of a splicing regulatory protein lacks a clear correlation with binding location (e.g. hnRNP L²⁰; SRSF1/2²⁶),

whereas in other cases RNA binding proteins have exhibited predictive position-dependent effects on splicing outcome (e.g., Nova²⁷; RbFox²⁸; MBNL²⁹). Here we use CLIP-Seq to identify the transcriptome-wide sites of CELF2 association in Jurkat T cells and correlate these sites of binding with the regulation of exon inclusion by CELF2 in the same cells. We find a clear correlation between binding location of CELF2 and its enhancement or repression of exon inclusion, in which binding of CELF2 to proximal intronic sequences upstream of a variable exon tracks with exon repression while binding of CELF2 to the downstream proximal intron enhances exon inclusion (Fig. 7A).

Our observed correlation between binding location and function of CELF2 in Jurkat T cells is consistent with previous mechanistic studies of CELF2 function on individual genes from muscle and neuron.^{15,19,30} For example, a study investigating how CELF2 activates exon inclusion suggested that binding of CELF2 downstream of an alternative exon stabilizes the association of the U2 snRNP component of the spliceosome with the upstream branch point region through direct interaction of

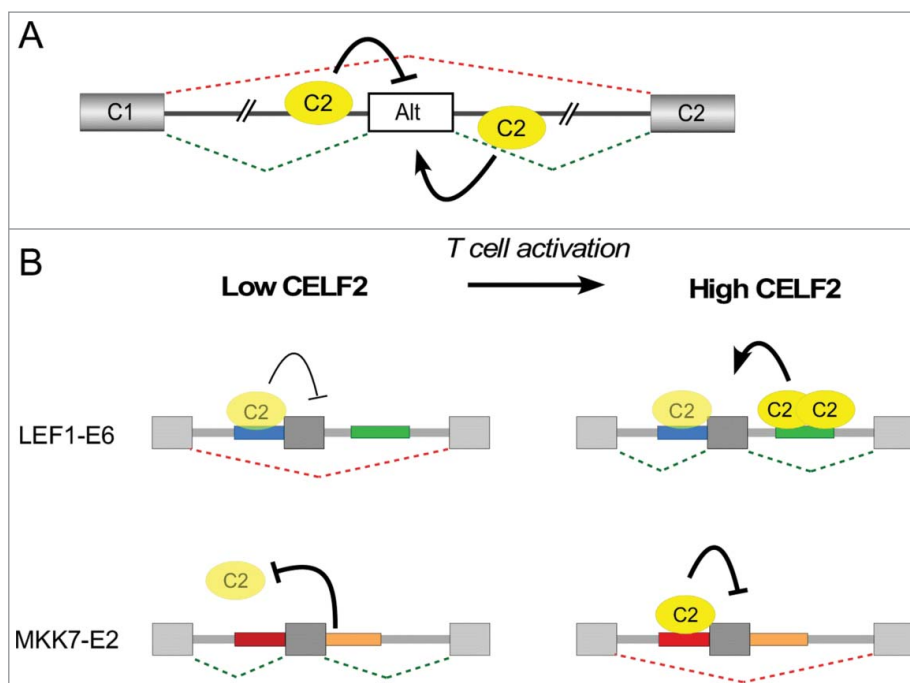


Figure 7. Model of position-dependent activity of CELF2 (A) Generalized position specific-activity of CELF2 as determined by overlap of CELF2 CLIP and splicing outcome. Colors and notations as in Fig. 2. (B) Summary of the binding and activity of CELF2 with respect to LEF1-E6 and MKK7-E2 under conditions of low CELF2 (unstimulated T cells) and high CELF2 (stimulated T cells). Coloring of schematics as in Figs. 4–6.

CELF2 with U2 snRNP proteins.¹⁹ Such a model would be consistent with the activity we observe when CELF2 binds to the DSE of LEF1-E6 and with the general pattern of downstream binding of CELF2 correlating with enhancement of exon inclusion. By contrast, CELF2 binding upstream of an alternative exon has been shown to repress exon inclusion by displacing the association of U2AF65 through binding to the perimeter of the branch point sequences.^{15,30} The binding of U2AF65 is a pre-requisite to the binding of U2 snRNP at branch point sequences to promote final spliceosome assembly. Inhibition of U2AF65 and/or U2 snRNP association by binding of CELF2 upstream of an alternative exon is also consistent with our “map” in Fig. 2B and would account for the activity we observe for LEF1-E6 and MKK7-E2 when CELF2 is bound to the USE or upstream intron respectively.

Importantly, the similarity between our correlation of binding and function of CELF2 in Jurkat T cells, and previous studies in neurons and muscle, suggests that CELF2 has intrinsic position-specific activity that is conserved across cell types. Intriguingly, a similar correlation between binding position and splicing outcome has been seen in a number of other tissue-specific splicing regulators (e.g. Nova, RbFox, MBNL^{27–29}). However, CELF2 is unique among these other factors in that the bioinformatic signals is strongest for the association of upstream binding with repression of exon inclusion, while for Nova, RbFox and MBNL the strongest association is typically between downstream binding and exon enhancement. Finally, our results also distinguish CELF2 from a recent global study of CELF1 in murine heart and muscle that found strongest association between exonic binding and repression,³¹ although a small scale study of CELF1 in C2C12 cells found a similar correlation between binding and splicing to what we describe here for CELF2.³²

Importantly for T cell function, the position-dependent activity of CELF2 suggested by the overlap of CLIP and functional data is sufficient to account for the activity of CELF2 in regulating 2 physiologically relevant targets in T cells, LEF1 and MKK7 (Fig. 7B). Specifically, in the case of LEF1 we observe that although both the USE and DSE bind CELF2, these elements and the bound CELF2 function antagonistically to each other. The USE is a repressor of splicing (Fig. 4A, B) and is bound by CELF2 in unstimulated T cells in which CELF2 expression is low (Fig. 5A, B). Consistently, CELF2 functions as a repressor of LEF1-E6 inclusion in unstimulated cells (Fig. 5C). Conversely, when CELF2 expression is increased upon stimulation, CELF2 binding is uniquely increased on the DSE, which functions as a splicing activator (Figs. 4, 5). As expected, knock-down studies confirm that CELF2 functions as an enhancer of LEF1-E6 in stimulated cells (Fig. 5C). By contrast, CELF2 represses MKK7-E2 inclusion in stimulated cells.¹⁸ This repression is consistent with the determination here that CELF2 binds exclusively to the intron upstream of MKK7-E2 (Fig. 6, 7B). Interestingly, for both LEF1 and MKK7 the change in splicing observed between unstimulated and stimulated conditions are attributable to a stimulation-induced change in CELF2 binding to the relevant introns. Some of this difference in binding is a result of increased CELF2 expression upon stimulation, however, further studies are needed to understand the mechanism by which the downstream intron in MKK7 represses CELF2 binding to the upstream intron in unstimulated cells and why the DSE is favored over the USE for CELF2 binding in stimulated cells.

In addition to revealing important insight into the function of CELF2 as a splicing regulatory protein, our CLIP-Seq data also suggest additional roles of CELF2 in RNA processing. Most notably, the enrichment of CELF2 for 3'UTR interactions

is potential evidence of a broader role for CELF2 in 3' end processing or splicing within 3' UTRs. A recent CLIP-seq analysis of CELF1 in mouse cardiac tissue similarly identified enrichment of CELF1 CLIP-seq peaks within 3'UTRs.³¹ CELF1, a related RNA binding protein from the same Elav-like factor family (CELF family), binds to UG-rich elements in the 3'UTRs of human mRNAs to trigger mRNA decay.³³ A few previous studies have suggested a role of CELF2 in the control of translation and/or cytoplasmic mRNA stability¹¹; however, unlike CELF1 that is expressed in both the nucleus and cytoplasm of Jurkat cells, CELF2 appears to be largely or exclusively nuclear.⁷ Therefore, CELF2 and CELF1 likely impact distinct steps in RNA processing and lifespan although perhaps through binding to similar sequences. Further work outside the scope of this study will be required to determine the functional significance of the 3'UTR association of CELF2.

In sum, this study provides evidence for a generalized position-dependent activity of CELF2 in splicing that can be used to predict its consequence on alternative splicing in a cell-type independent manner. We also provide further insight into the mechanism by which the splicing of LEF1 and MKK7 are regulated in human T cells to alter transcriptional (LEF1) and signaling (MKK7) pathways. Finally, our data suggests that alternative splicing is not the only step in RNA biogenesis influenced by CELF2. On the other hand, the lack of enriched CELF2 binding to intergenic regions or distal introns implies that mRNA processing is the predominant cellular function of CELF2. Further studies will be of interest to expand on these findings and uncover additional layers of regulation of and by CELF2.

Materials and methods

Cell culture

JSL1 Jurkat cells²¹ were cultured in RPMI+ 5% fetal calf serum at 37°C in 5% CO₂. Sub-lines of JSL1 cells that stably express the minigenes described were created by transfecting 10 million cells with 10 ug of minigene plasmid by electroporation and grown under drug selection as described by.³⁴ For splicing analysis, 3 independent clones of each minigene were either left untreated or treated with 20 ng/ml of PMA for 60 h, after which cells were harvested and total RNA extracted using RNABee (Tel-Test). Minigene derived spliced products were analyzed by RT PCR using vector-specific primers (see below). Knock-down of CELF2 was done using lentiviral expressed shRNAs as described previously.^{6,18}

CLIP-seq

JSL1 cells were cultured in RPMI medium containing 5% Fetal Bovine Serum at 37°C in 5% CO₂ for 60 hours, or stimulated with 20 ng/ml phorbol myristate acetate (PMA) for 60 hours. CLIP was carried out as we have described previously.^{23,24} Briefly, unstimulated and stimulated cells were washed twice with Hank's Balanced Salt Solution (HBSS), and subjected to UV-crosslinking on ice. Cells were lysed, treated with DNase, and RNase T1, and immuno-precipitated using Protein-G sepharose beads coated with anti-CELF2 antibody (University

of Florida Hybridoma Lab HL1889). After stringent washing, radioactive 3' RNA linker was ligated to RNA cross-linked to protein, and samples resolved on 10% Bis-Tris Novex NuPAGE gels. The RNA bound to CELF2 was eluted from the membrane by proteinase K/7M Urea, ligated to 5' RNA linker, and cDNA synthesized. The library was prepared from the cDNA samples using a 2-step PCR reaction. Prior to the first PCR step each sample was split into 3 and separate bar-codes were incorporated during the second PCR step for high throughput sequencing. Individually bar-coded sequencing libraries were pooled and sequenced on an Illumina Hi-Seq 2000 at the University of Pennsylvania Next Generation Sequencing Core (NGSC). The division of each sample into separate bar-coded samples allowed us to gain greater depth as we could distinguish PCR artifact from identical crosslinked RNA species in the subsequent analysis.

CLIP-seq data analysis

Raw reads were first trimmed from the 3' end for basecall quality of 0 (PHRED score). Sequencing adaptors were removed using cutadapt 0.9.4 and homopolymeric runs ≥ 6 nt were trimmed from the 3' end. Reads were aligned to hg19 with bowtie 0.12.7, allowing for a maximum of 2 mismatches between the read and the index. Alignments were filtered for unambiguous mapping and duplicate alignments (start and end coordinate within the same bar-coded sample) were removed before calling peaks (Supplemental Table 1). Replicates were combined, allowing duplicate alignments only where they originated in separately barcoded and sequenced samples. Peaks were called empirically using an FDR threshold of 0.001, comparing CLIP signal to backgrounds generated from 100 permutations of CLIP tags within bound transcripts (as described in ref. 23). RefSeq mRNAs were searched for peaks, and peaks within 50 nts were merged into binding sites. Binding sites with support from fewer than 2 replicates were discarded from further analysis.

Motif enrichment analysis

Z-scores were assigned to each of the 4,096 possible hexamers observed within binding sites based on 100 permutations of the positions of binding sites within bound transcripts. The top 20 hexamers were aligned with ClustalW2 to generate sequence logos with WebLogo 2.8.³⁵

Definition of CELF2 regulated and CELF2 bound events

CELF2 regulated exons were defined using previously published data⁶ using thresholds shown to yield high validation rates across many experimental contexts in this system.^{6,18,20,36} Briefly, we first calculated a Δ PSI (change in Percent Spliced In) for alternative exons in WT vs. CELF2 depleted cells. Events were considered enhanced by CELF2 if upon depletion Δ PSI < -10 with $p < 0.05$ or repressed by CELF2 if Δ PSI > 10 with $p < 0.05$ in either unstimulated or stimulated JSL1 cells. Exons were considered bound and regulated if the above conditions were met and there was a CELF2 CLIP peak present in the specified region(s)

in the context in which it was regulated. CELF2 unresponsive exons were defined as those with $|\Delta\text{PSI}| < 3$ and $p > 0.05$ in both unstimulated and stimulated cells and had no overlap with a CELF2 regulated exon. Exons were considered bound and unresponsive if the above conditions were met and there was a CLIP peak in the specified region(s) in either unstimulated or stimulated cells.

Conservation analysis

The human phastCons46way placental mammal conservation track was downloaded from the UCSC genome browser and scores were extracted for all alternative exons queried by RASL-seq that were expressed in JSL1 cells. Different subsets of exons were defined based on CELF2 regulation and/or binding status within 300 nt upstream or downstream of these exons and the average score per nucleotide was plotted using a running mean of 5-nt centered at each position.

Gene ontology analysis

We analyzed enriched GO terms (GO_FAT for Molecular Function and Biological Process) using DAVID ver. 6.7 (<http://david.abcc.ncifcrf.gov/>) comparing genes with a CELF2 CLIP peak in at least one of 3 regions proximal to RefSeq internal exons (within 300 nt upstream, within 300 nt downstream, or within the exon) or genes bound by CELF2 elsewhere (e.g., distal intronic or UTR regions) to all transcripts expressed in JSL1 cells, as defined by RNA-seq.²⁰ After applying a Bonferroni correction for multiple hypothesis tests, the $-\log(p\text{-value})$ of the 70 terms that had a significant enrichment ($p < 0.05$) in at least one of these 4 regions were clustered using a Euclidean distance metric.

Minigenes and RNA

The USE/DSE, alt60/DSE, USE/alt120 minigenes, consisting of LEF1 exon 6 and surrounding intron regions flanked by intron and exon sequence from the human β -globin gene, were previously described in.⁷ Alt-both was made using PCR by using the alt60 and alt120 sequences to replace the USE and DSE in the same construct. 1x-4x UGUU minigenes were made using synthetic oligos for the 1xUGUU sequence (GUGC(UUUUCU)GUUGUUGUUGU) with added restriction enzyme sites to allow oligomerization. These were cloned into the WT minigene to replace the DSE120.

RNA corresponding to USE/DSE, Δ /DSE, alt60/DSE, USE/alt120, alt-both and Δ /alt120 were created by PCR with primers (with a T7 tag attached) to the respective minigene that contained the sequence. Similarly, 1x-4x UGUU were amplified from minigenes with primers with a T7 tag attached using PCR and used as templates for in vitro transcription. The RNAs were transcribed with T7 polymerase (Promega) in the absence or presence of ³²P-UTP to radioactively label probes. MKK7 RNAs were similarly transcribed with T7 polymerase from templates generated by PCR amplification of sequences described in.¹⁸

Nuclear extract and recombinant proteins

Nuclear extract was purified from JSL1 cells grown under unstimulated or stimulated conditions (50 ng/ml PMA) using a standard protocol previously described in ref 37. Recombinant FLAG-tagged CELF2 was purified from nuclear extract prepared from JSL1 cells stably expressing FLAG-CELF2. Tagged protein was purified from nuclear extract with EZ-View Red FLAG-conjugated resin (Sigma) in GFB300 (20 mM Tris-Cl, pH 7.5, 300 mM KCl, and 0.2 mM EDTA, pH 8.0). Following extensive washing in GFB300, the proteins were eluted with 500 ng/ul of 3X Flag peptide (Sigma). Protease and Phosphatase inhibitor cocktails (Sigma) and de-acetylase inhibitor (Millipore) were used during the purification.

RT-PCR

RT-PCR and analysis was carried out as previously described in detail.³³ In brief, a low-cycle PCR protocol was used, such that the signal detected is linear with respect to input RNA. Minigenes were analyzed using the vector-specific primers ACT and GE3R (sequence published in ref 34). Quantitation was done by densitometry using a Typhoon Phosphorimager (Amersham Biosciences).

In vitro splicing assay

Unlabeled RNA substrates (10 nM) were incubated with 30% unstimulated JSL1 nuclear extract in a total volume of 12.5 μ l under splicing conditions, which contains (final concentration): 12 mM Tris-HCl, pH7.5, 3.2 mM MgCl₂, 4 mM ATP, 20 mM CP, 0.5 mM DTT, 0.125U RNasin (Promega), 60 mM KCl, 0.1 mM EDTA, and 12% glycerol. Reactions were incubated for 90 min at 30°C; then the RNA was recovered from the reactions by proteinase K treatment, phenol- chloroform extraction and EtOH precipitation. The recovered RNA was analyzed by RT-PCR.

UV Crosslinking

Radiolabeled RNA was incubated in JSL1 nuclear extract under similar conditions described for the EMSAs. Reactions were incubated for 20 min at 30°C, crosslinked using UV light (254 nm) for 20 min on ice, and digested with 2 μ g (final concentration) of RNase T1 and RNase A each for 20 min at 37°C. Reactions were analyzed under denaturing conditions on a 12% gel (Acrylamide/Bis 37.5:1, BioRad), and visualized by autoradiography. Immunoprecipitation following crosslinking was done as described in ref 18 using the following antibodies: CELF2 (UFI Hybridoma Lab, HL1889); HuR (Santa Cruz, sc-5261); hnRNP C (Abcam, ab10294); and hnRNP H (Abcam, ab10374).

RNA electro-mobility shift assays (EMSA)

In vitro transcribed RNAs were gel-purified and adjusted to 10⁴ cpm/ml specific activity. Each RNA was incubated with FLAG-CELF2 in a total volume of 10ul under splicing conditions similar to that described for the in vitro splicing assays

with the addition of 0.8 mg of BSA and 0.8 mg. Reactions were incubated for 20 min at 30°C, after which heparin was added to a final concentration of 5 mg/ml and incubated for an additional 5 min at 30°C. Reactions were analyzed on a 4.5% native gel (Acrylamide/Bis 29:1 BioRad) and visualized by autoradiography.

Accession numbers

Raw sequencing reads for all 12 biological samples in this study are available along with processed binding profiles under GEO accession number GSE71264 (BioProject accession PRJNA285907).

Disclosure of potential conflicts of interest

No potential conflicts of interest were disclosed.

Acknowledgments

We thank Yoseph Barash and current members of the Lynch lab for helpful discussions and advice, and thank Maurice Swanson and the hybridoma facility at the University of Florida for the CELF2 antibody.

Funding

This work was supported by the National Institutes of Health through grants R01GM103383 to KWL and F31GM103255 to NMM.

References

- Fu XD, Ares M Jr. Context-dependent control of alternative splicing by RNA-binding proteins. *Nat Rev Genet* 2014; 15:689-701; PMID:25112293; <http://dx.doi.org/10.1038/nrg3778>
- Martinez NM, Lynch KW. Control of alternative splicing in immune responses: many regulators, many predictions, much still to learn. *Immunol Rev* 2013; 253:216-36; PMID:23550649; <http://dx.doi.org/10.1111/imr.12047>
- Warzecha CC, Carstens RP. Complex changes in alternative pre-mRNA splicing play a central role in the epithelial-to-mesenchymal transition (EMT). *Semin Cancer Biol* 2012; 22:417-27; PMID:22548723; <http://dx.doi.org/10.1016/j.semcancer.2012.04.003>
- Black DL, Grabowski PJ. Alternative pre-mRNA splicing and neuronal function. *Prog Mol Subcell Biol* 2003; 31:187-216; PMID:12494767; http://dx.doi.org/10.1007/978-3-662-09728-1_7
- Cooper TA, Wan L, Dreyfuss G. RNA and disease. *Cell* 2009; 136:777-93; PMID:19239895; <http://dx.doi.org/10.1016/j.cell.2009.02.011>
- Mallory MJ, Allon SJ, Qiu J, Gazzara MR, Tapescu I, Martinez NM, Fu XD, Lynch KW. Induced transcription and stability of CELF2 mRNA drives widespread alternative splicing during T-cell signaling. *Proc Natl Acad Sci U S A* 2015; 112:E2139-48; PMID:25870297; <http://dx.doi.org/10.1073/pnas.1423695112>
- Mallory MJ, Jackson J, Weber B, Chi A, Heyd F, Lynch KW. Signal- and development-dependent alternative splicing of LEF1 in T cells is controlled by CELF2. *Mol Cell Biol* 2011; 31:2184-95; PMID:21444716; <http://dx.doi.org/10.1128/MCB.05170-11>
- Zhang W, Liu H, Han K, Grabowski PJ. Region-specific alternative splicing in the nervous system: implications for regulation by the RNA-binding protein NAPOR. *RNA* 2002; 8:671-85; PMID:12022233; <http://dx.doi.org/10.1017/S1355838202027036>
- Ladd AN, Charlet N, Cooper TA. The CELF family of RNA binding proteins is implicated in cell-specific and developmentally regulated alternative splicing. *Mol Cell Biol* 2001; 21:1285-96; PMID:11158314; <http://dx.doi.org/10.1128/MCB.21.4.1285-1296.2001>
- Kalsotra A, Xiao X, Ward AJ, Castle JC, Johnson JM, Burge CB, Cooper TA. A postnatal switch of CELF and MBNL proteins reprograms alternative splicing in the developing heart. *Proc Natl Acad Sci U S A* 2008; 105:20333-8; PMID:19075228; <http://dx.doi.org/10.1073/pnas.0809045105>
- Dasgupta T, Ladd AN. The importance of CELF control: molecular and biological roles of the CUG-BP, Elav-like family of RNA-binding proteins. *Wiley Interdiscip Rev RNA* 2011; 3:104-21; PMID:22180311; <http://dx.doi.org/10.1002/wrna.107>
- Kalsotra A, Wang K, Li PF, Cooper TA. MicroRNAs coordinate an alternative splicing network during mouse postnatal heart development. *Genes Dev* 2010; 24:653-8; PMID:20299448; <http://dx.doi.org/10.1101/gad.1894310>
- Han J, Cooper TA. Identification of CELF splicing activation and repression domains in vivo. *Nucleic Acids Res* 2005; 33:2769-80; PMID:15894795; <http://dx.doi.org/10.1093/nar/gki561>
- Singh G, Charlet BN, Han J, Cooper TA. ETR-3 and CELF4 protein domains required for RNA binding and splicing activity in vivo. *Nucleic Acids Res* 2004; 32:1232-41; PMID:14973222; <http://dx.doi.org/10.1093/nar/gkh275>
- Dujardin G, Buratti E, Charlet-Berguerand N, Martins de Araujo M, Mbopda A, Le Jossic-Corcoc C, Pagani F, Ferec C, Corcos L. CELF proteins regulate CFTR pre-mRNA splicing: essential role of the divergent domain of ETR-3. *Nucleic Acids Res* 2010; 38:7273-85; PMID:20631008; <http://dx.doi.org/10.1093/nar/gkq573>
- Blech-Hermoni Y, Stillwagon SJ, Ladd AN. Diversity and conservation of CELF1 and CELF2 RNA and protein expression patterns during embryonic development. *Dev Dyn* 2013; 242:767-77; PMID:23468433; <http://dx.doi.org/10.1002/dvdy.23959>
- McAuliffe JJ, Gao LZ, Solaro RJ. Changes in myofibrillar activation and troponin C Ca²⁺ binding associated with troponin T isoform switching in developing rabbit heart. *Circ Res* 1990; 66:1204-16; PMID:2139820; <http://dx.doi.org/10.1161/01.RES.66.5.1204>
- Martinez NM, Agosto L, Qiu J, Mallory MJ, Gazzara MR, Barash Y, Fu XD, Lynch KW. Widespread JNK-dependent alternative splicing induces a positive feedback loop through CELF2-mediated regulation of MKK7 during T-cell activation. *Genes Dev* 2015; 29:2054-66; PMID:26443849; <http://dx.doi.org/10.1101/gad.267245.115>
- Goo YH, Cooper TA. CUGBP2 directly interacts with U2 17S snRNP components and promotes U2 snRNA binding to cardiac troponin T pre-mRNA. *Nucleic Acids Res* 2009; 37:4275-86; PMID:19443441; <http://dx.doi.org/10.1093/nar/gkp346>
- Cole BS, Tapescu I, Allon SJ, Mallory MJ, Qiu J, Lake RJ, Fan HY, Fu XD, Lynch KW. Global analysis of physical and functional RNA targets of hnRNP L reveals distinct sequence and epigenetic features of repressed and enhanced exons. *RNA* 2015; 21:2053-66; PMID:26437669; <http://dx.doi.org/10.1261/rna.052969.115>
- Lynch KW, Weiss A. A model system for the activation-induced alternative-splicing of CD45 implicates protein kinase C and Ras. *Mol Cell Biol* 2000; 20:70-80; PMID:10594010; <http://dx.doi.org/10.1128/MCB.20.1.70-80.2000>
- Ule J, Jensen K, Mele A, Darnell RB. CLIP: a method for identifying protein-RNA interaction sites in living cells. *Methods* 2005; 37:376-86; PMID:16314267; <http://dx.doi.org/10.1016/j.ymeth.2005.07.018>
- Shankarling G, Cole BS, Mallory MJ, Lynch KW. Transcriptome-wide RNA interaction profiling reveals physical and functional targets of hnRNP L in human T cells. *Mol Cell Biol* 2014; 34:71-83; PMID:24164894; <http://dx.doi.org/10.1128/MCB.00740-13>
- Moy RH, Cole BS, Yasunaga A, Gold B, Shankarling G, Varble A, Molleston JM, tenOever BR, Lynch KW, Cherry S. Stem-loop recognition by DDX17 facilitates miRNA processing and antiviral defense. *Cell* 2014; 158:764-77; PMID:25126784; <http://dx.doi.org/10.1016/j.cell.2014.06.023>
- Faustino NA, Cooper TA. Identification of putative new splicing targets for ETR-3 using sequences identified by systematic evolution of ligands by exponential enrichment. *Mol Cell Biol* 2005; 25:879-87; PMID:15657417; <http://dx.doi.org/10.1128/MCB.25.3.879-887.2005>
- Pandit S, Zhou Y, Shiue L, Coutinho-Mansfield G, Li H, Qiu J, Huang J, Yeo GW, Ares M Jr, Fu XD. Genome-wide analysis reveals SR protein cooperation and competition in regulated

- splicing. *Mol Cell* 2013; 50:223-35; PMID:23562324; <http://dx.doi.org/10.1016/j.molcel.2013.03.001>
27. Ule J, Stefani G, Mele A, Ruggiu M, Wang X, Taneri B, Gaasterland T, Blencowe BJ, Darnell RB. An RNA map predicting Nova-dependent splicing regulation. *Nature* 2006; 444:580-6; PMID:17065982; <http://dx.doi.org/10.1038/nature05304>
 28. Lovci MT, Ghanem D, Marr H, Arnold J, Gee S, Parra M, Liang TY, Stark TJ, Gehman LT, Hoon S, et al. Rbfox proteins regulate alternative mRNA splicing through evolutionarily conserved RNA bridges. *Nat Struct Mol Biol* 2013; 20:1434-42; PMID:24213538; <http://dx.doi.org/10.1038/nsmb.2699>
 29. Wang ET, Cody NA, Jog S, Biancolella M, Wang TT, Treacy DJ, Luo S, Schroth GP, Housman DE, Reddy S, et al. Transcriptome-wide regulation of pre-mRNA splicing and mRNA localization by muscleblind proteins. *Cell* 2012; 150:710-24; PMID:22901804; <http://dx.doi.org/10.1016/j.cell.2012.06.041>
 30. Dembowski JA, Grabowski PJ. The CUGBP2 splicing factor regulates an ensemble of branchpoints from perimeter binding sites with implications for autoregulation. *PLoS Genet* 2009; 5:e1000595; PMID:19680430; <http://dx.doi.org/10.1371/journal.pgen.1000595>
 31. Wang ET, Ward AJ, Cherone JM, Giudice J, Wang TT, Treacy DJ, Lambert NJ, Freese P, Saxena T, Cooper TA, et al. Antagonistic regulation of mRNA expression and splicing by CELF and MBNL proteins. *Genome Res* 2015; 25:858-71; PMID:25883322; <http://dx.doi.org/10.1101/gr.184390.114>
 32. Masuda A, Andersen HS, Doktor TK, Okamoto T, Ito M, Andresen BS, Ohno K. CUGBP1 and MBNL1 preferentially bind to 3' UTRs and facilitate mRNA decay. *Sci Rep* 2012; 2:209; PMID:22355723; <http://dx.doi.org/10.1038/srep00209>
 33. Vlasova IA, Tahoe NM, Fan D, Larsson O, Rattenbacher B, Sternjohn JR, Vasdewani J, Karypis G, Reilly CS, Bitterman PB, et al. Conserved GU-rich elements mediate mRNA decay by binding to CUG-binding protein 1. *Mol Cell* 2008; 29:263-70; PMID:18243120; <http://dx.doi.org/10.1016/j.molcel.2007.11.024>
 34. Rothrock C, Cannon B, Hahm B, Lynch KW. A conserved signal-responsive sequence mediates activation-induced alternative splicing of CD45. *Mol Cell* 2003; 12:1317-24; PMID:14636588; [http://dx.doi.org/10.1016/S1097-2765\(03\)00434-9](http://dx.doi.org/10.1016/S1097-2765(03)00434-9)
 35. Crooks GE, Hon G, Chandonia JM, Brenner SE. WebLogo: a sequence logo generator. *Genome Res* 2004; 14:1188-90; PMID:15173120; <http://dx.doi.org/10.1101/gr.849004>
 36. Yarosh CA, Tapescu I, Thompson MG, Qiu J, Mallory MJ, Fu XD, Lynch KW. TRAP150 interacts with the RNA-binding domain of PSF and antagonizes splicing of numerous PSF-target genes in T cells. *Nucleic Acids Res* 2015; 43:9006-16; PMID:26261210; <http://dx.doi.org/10.1093/nar/gkv816>
 37. Lynch KW, Weiss A. A CD45 polymorphism associated with Multiple Sclerosis disrupts an exonic splicing silencer. *J Biol Chem* 2001; 276:24341-7; PMID:11306584; <http://dx.doi.org/10.1074/jbc.M102175200>